Chemical Shifts in X-ray and Photo-Electron Spectroscopy: A Historical review

Ingvar Lindgren*
Department of Physics, Chalmers University of Technology
and Göteborg University, Göteborg, Sweden

Contents

Abstract

A review with historical emphasis is given of the discovery and evaluation of chemical shifts in X-ray and photo-electron spectroscopy. The discovery and interpretation of the shifts in the X-ray spectra in the early 1920's are treated as an introduction and general background. The discovery of the shifts in photo-electron spectra, discovered in the late 1950's, and its interpretation, which led to the invention of the ESCA method – *Electron Spectroscopy for Chemical Analysis* – in the early 1960's, are then reviewed. Various methods of evaluating the core-electron binding energies and chemical shift are discussed – from atomic self-consistent-field calculations in the early 1960's to quite sophisticated many-body and density-functional calculation in the late 1990's.

*ingvar.lindgren@fy.chalmers.se

1 Introduction

sec:Intro

At the ICESS-9 *Conference on Electronic Spectroscopy and Structure*, which is celebrating the 40:th anniversary of the ESCA method – *Electron Spectroscopy for Chemical Analysis* – and at the same time the 85:th birthday of the inventor Kai Siegbahn, I have been asked to give a review with historical emphasis of the chemical shifts in electron spectroscopy. I will start this with a short review of the discovery and interpretation of the chemical shifts in X-ray spectroscopy. This effect was discovered in the early 1920's, and the interpretations given at this early date were essentially correct. The effect is the same as that causing the chemical shifts in electron spectroscopy.

The X-ray spectroscopy started with the early works of Barkla, Bragg and others around 1915, and the experimental technique was then greatly refined, particularly by Manne Siegbahn and his collaborators in Lund and Uppsala and later in Stockholm [1]. Manne Siegbahn received the Nobel prize in physics for his achievements.

Sieg31

With particular regard to the subject of this review, it is interesting to cite a paragraph from Manne Siegbahn's Nobel lecture: *'Recently, in a lecture to the Swedish society of Chemists, I drew attention to preliminary studies which are being made in one of these new fields - the matter of the chemical properties of the atoms having an effect upon the phenomenon of X-radiation.'*

This was a great surprise at the time, since it was generally accepted that the X-radiation was a purely atomic effect. These early discoveries seem to have been largely overlooked by later generations of spectroscopists.

2 Chemical shift in X-ray spectroscopy

sec:X-ray

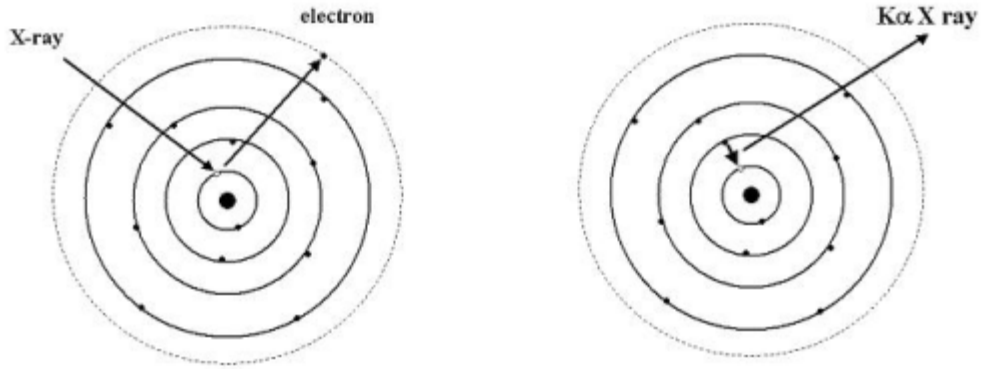

Figure 1: The excitation by continuous X-radiation of an inner electron to the lowest available level leads to an 'absorption edge' (left). An inner electron vacancy can be refilled by an electron from an outer shell, which leads to chacteristic X-radiation (right).

Fig:AbsEmis

When an atom is irradiated by an energetic beam of particles or photons, an electron from an inner shell can be expelled (see Fig.1). When the vacancy is filled by an electron from an outer electronic shell, so called *characteristic X-ray radiation* can be emitted. The energy of the radiation depends on the energy levels of the atom. If an atom is irradiated by *continuous* X-rays, then the radiation can be absorbed if the energy of the incoming photon is sufficient to ionize the atom or to excite the inner electron to an unoccupied level. This gives rise to an *absorption edge* in the spectrum for each inner level.

Fig:AbsEmis

Table 1: K-absorption edge in chlorine
(From A.Lindh 1921 [2],[1, p. 280])

Compound	Edge (XU)	Shift (eV)
Cl_2	4393.8	0
HCl	4385.3	5.4
Val.1	4382.9	7.0
Val.5	4376.9	10.9
Val.7	4369.8	15.5

Tab:Lindh

The position of the absorption edge gives information about the electron binding energy, i.e., the energy needed to remove the electron from the atom. One problem is here that the edge has a certain structure, which makes the determination of the absolute binding energy difficult (see Fig.2). The emission spectrum, on the other hand, gives information about the *difference* in binding energy between different shells – a quantity that could be determined with higher accuracy. For several decades, X-ray spectroscopy was the main source of information regarding the atomic structure. (For an extensive review of the early X-ray spectroscopy, the reader is referred to the monograph by Manne Siegbahn [1]).

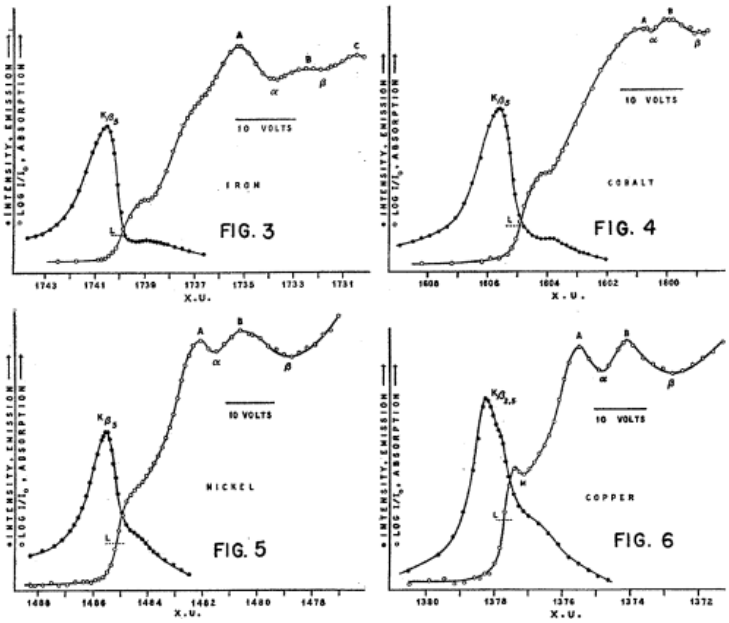

Figure 2: The X-ray absorption edge has a pronounced 'fine structure', which makes the interpretation difficult.

Fig:AbsEdge

2.1 Discovery of the chemical shift in X-ray spectroscopy

In the early 1920's it was discovered that the wavelengths of the X-radiation and the position of the absorption edge depend on the chemical environment of the atom. Bergengren [3] of the Manne Siegbahn group at the university of Lund found in 1920 that the K-absorption spectrum was different for different modifications of phosphorus. In 1921

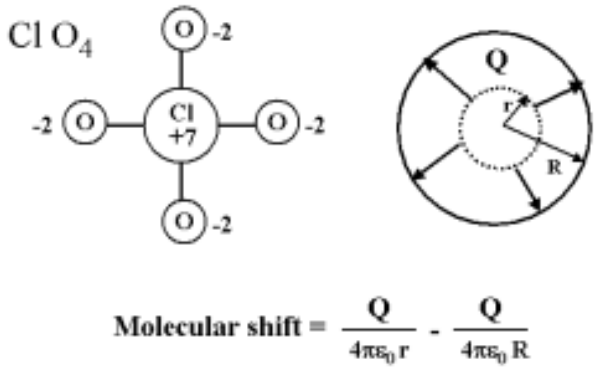

Figure 3: In the model of Wenzel [8] and Coster [9] an effective charge (Q) is transferred from the central atom to an outer spherical shell, representing the surrounding atoms of the molecule.

Fig:Interpret

Lindh [2] of the same group found that the position of the X-ray absorption edge of chlorine depends on the *chemical valence* (see 1). Then the *chemical shift* in X-ray absorption was discovered.

Table 2: Chemical shifts in X-ray emission
(From E.Bäcklin 1925 [4], [1, p. 280])

Compound	Shift (eV)
Al-Al_2O_3	0.31
Si-SiO_2	0.57
P-P_2O_5	0.89
S-Ba_2SO_4	1.31

Tab:Back

That also the wavelength of the X-ray emission lines depends on the chemical environment was discovered in the mid 1920's by Lindh and Lundquist [5, 6], Ray [7], and Bäcklin [4]. Some results obtained by Bäcklin are shown in Table 2.

2.2 Interpretation of the chemical shift in X-ray spectroscopy

ec:Interpret

The main cause of the chemical shifts in the X-ray absorption spectrum was realized already in the early 1920's. A model developed by Wenzel [8] and Coster [9] is illustrated for the chlorate ion in Fig.3. Here, the valence of the chlorine ion is +7 and of the surrounding oxygen ions -2. If a certain charge (Q) of the central ion, assumed to be distributed uniformly on a sphere of radius r, is removed to infinity, the potential inside that shell would be changed by $Q/4\pi\epsilon_o r$ – and hence the binding energy of electrons inside the shell by the same amount. In reality the charge is mainly transferred to the surrounding ions, and assuming that these can be represented by a uniformly charged spherical shell of radius R, the effective energy shift would be

$$\Delta E = \frac{Q}{4\pi\epsilon_0}\Big(\frac{1}{r} - \frac{1}{R}\Big).$$

Since the molecular bonds are generally not purely ionic but at least partly covalent, the effective charge is considerably smaller than the valence numbers would indicate.

This simple model gives a qualitative explanation of the shift in the binding energy and hence of the X-ray absorption edge. Since the potential is constant inside a uniformly charged spherical shell, this model does not provide any explanation of the shift observed in the X-ray emission spectra.

3 Chemical shift in photo-electron spectroscopy

sec:PhotoEl

3.1 Invention of the high-resolution electron spectroscopy

sec:InvElSp

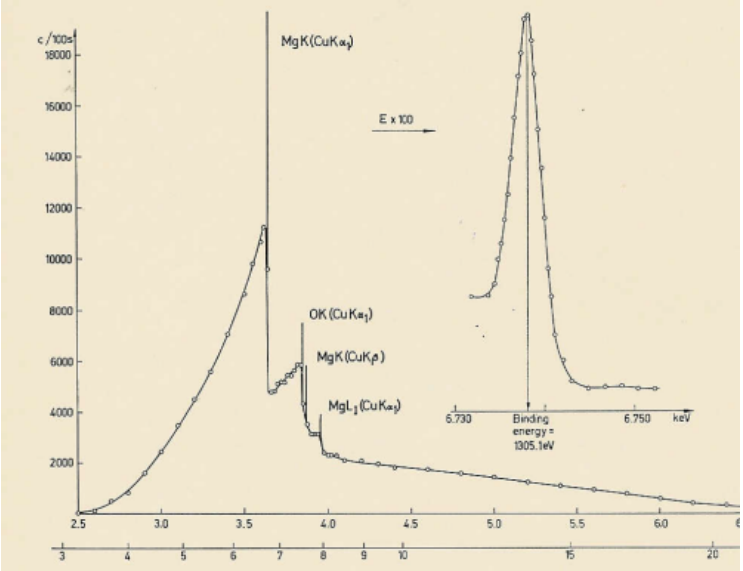

Figure 4: An early high-resolution photo-electron spectrum. Note the very sharp line at the peak of the spectrum – magnified 100 times to the right – which corresponds to electrons with zero energy loss. (From the first ESCA book [10, p.11]).

ESCA67

Fig:ESCASpect

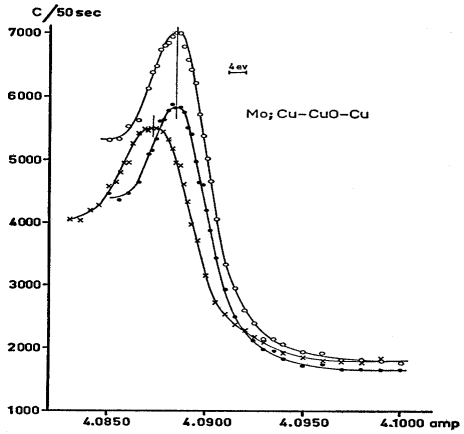

Figure 5: The shift in 1s binding energy of copper between Cu metal and CuO (from Sokolowski, Nordling, and Siegbahn 1958 [11]).

SNS58

Fig:Copper

In photo-electron spectroscopy an electron is expelled by monochromatic X-ray or UV radiation ($h\nu$), and the kinetic energy (E_{kin}) of the expelled electron is measured by an

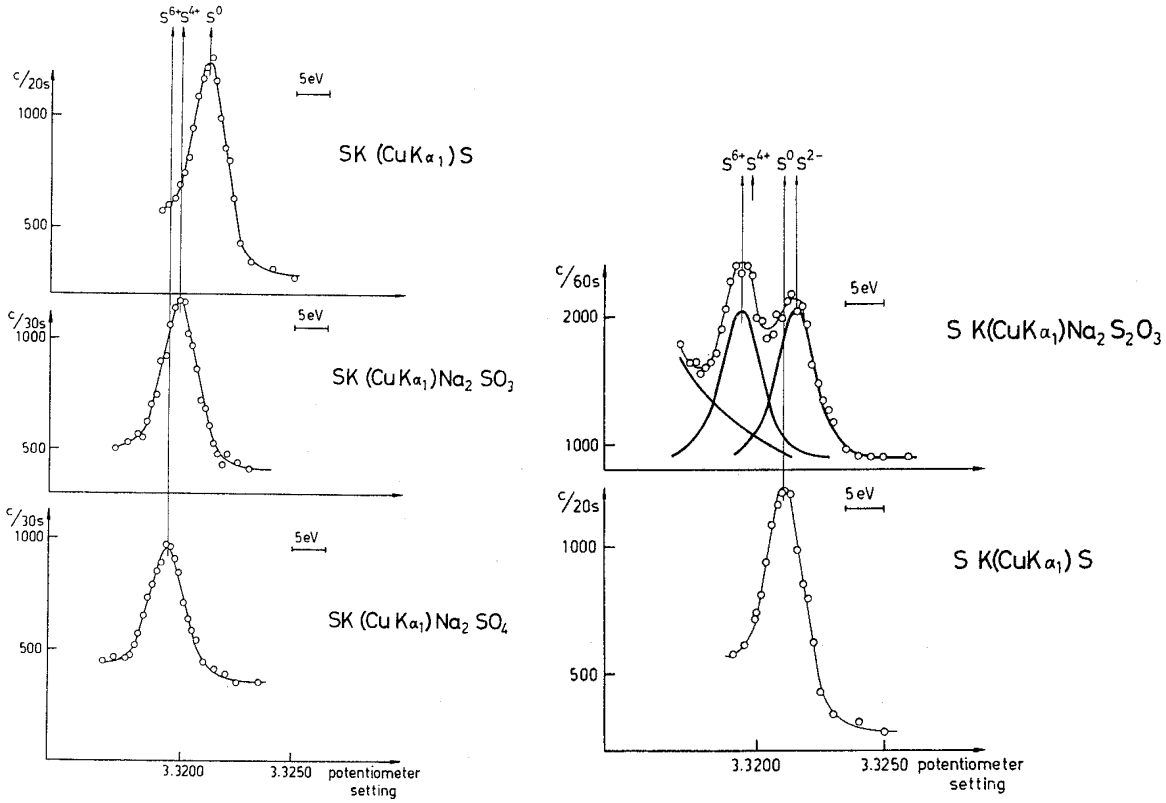

Figure 6: The chemical shift between pure sulfur and some sulfur compounds (left) and the spectrom of sulfur thiosulfate (right) (from Hagström, Nordling and Siegbahn 1964 [12]). HNS64 Fig:Sulfur

electron spectrometer. The binding energy of the electron is then simply given by the relation

$$\mathrm{BE} = \mathrm{h}\nu - \mathrm{E}_{\mathrm{kin}}.$$

(This yields the binding energy relative the Fermi level of the spectrometer, and a correction has to be applied to obtain the true binding energy.)

An early high-resolution photo-electron (ESCA) spectrum with X-ray radiation is shown in Fig.4. Fig:ESCASpect It illustrates the important discovery made in the late 1950's that the spectrum contains very sharp lines [13] NSS57 – in the early works of the order of a few eV but later found to be considerably sharper. One might expect that the lines would be broadened due to scattering in the target material. The energy losses experienced by the electrons on their way through the material, however, is quantized – *discrete energy losses* – and this implies that there is a finite probability that the electrons are expelled without any energy loss at all. This leads to a very sharp line – in principle, limited only by the natural line width. The phenomenon is quite analogous to the Mössbauer effect in the nuclear spectroscopy. This discovery opened the way for a new precision electron spectroscopy.

During the first years, the main emphasis of the new spectroscopy was to determine the electron binding energies in various atoms, and essentially all atoms were studied in this way (see the first ESCA book [10, App.5]) ESCA67. The precision is here considerably higher than in the X-ray-absorption method (c.f. Fig.2). Fig:AbsEdge

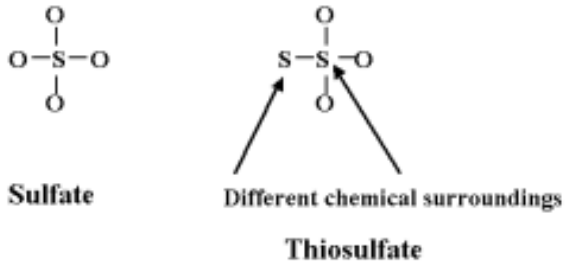

Figure 7: The thiosulfate ion contains two sulfur ions at inequivalent posistions, which leads to a double peak in the ESCA spectrum. Fig:Thiosulfate

3.2 Discovery of the chemical shift in photo-electron spectroscopy

In studying the electron binding energy, it was soon discovered that this energy does depend on the chemical environment of the atom studied. The first observation of that effect was made in 1957 by Sokolowski, Nordling, and Siegbahn [11], SNS58 where a shift of several eV was found between metallic copper and copper oxide (se Fig.5). Fig:Copper The effect was even more pronounced for elements like chlorine or sulfur, which can appear in a number of different environments. The shift of some sulfur compounds is illustrated in Fig.6. Fig:Sulfur Although this effect is quite analogous to the corresponding shift in X-ray absorption, discovered more than three decades earlier, it came as a surprise to the investigators, and the interpretation was unclear for some time – possible surface charge was one hypothetical explanation.

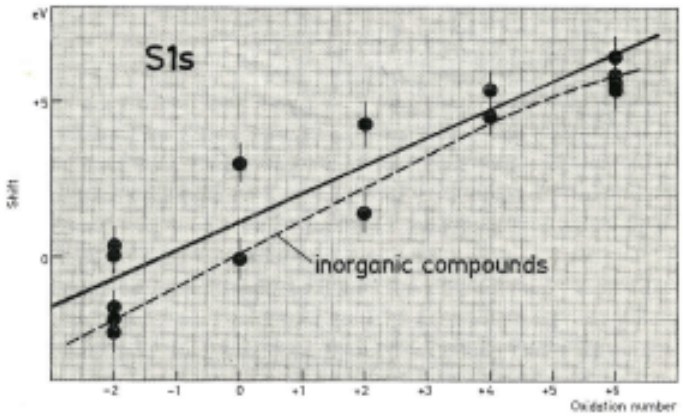

Figure 8: The experimental shift of the sulfur compounds versus the chemical valence or oxidation number (from the first ESCA book [10, p.101]). ESCA67 Fig:ShiftS1

A remarkable and crucial discovery was made on the Christmas Eve of 1963 – or possibly the day before, the reports from the participants are here slightly diverging. The Uppsala group, Hagström, Nordberg, Nordling, was making some complementary measurements on sulfur but was running out of the compounds normally used (sulfate or sulfite). They knew that a sulfur compound was used in the photographic process and therefore borrowed some salt from the photo lab. Then to their big surprise a *double peak* showed up in the spectrum [12] HNS64 (see Fig.6, right). Fig:Sulfur This effect was real and could not be due to any (irregular) surface charge or other instrumental effect, since the sodium 1*s* line was still unsplit. The salt used was thiosulfate, which contains two sulfur ions at different

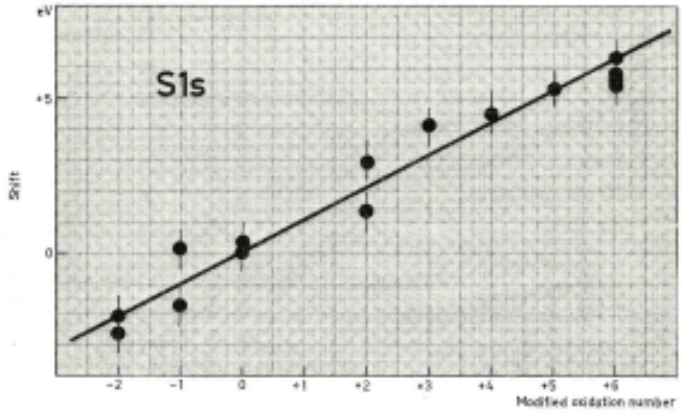

Figure 9: The experimental shift of the sulfur compounds versus the 'modified oxidation number', explained in the text (from the first ESCA book [10, p.101]).

Fig:ShiftS2

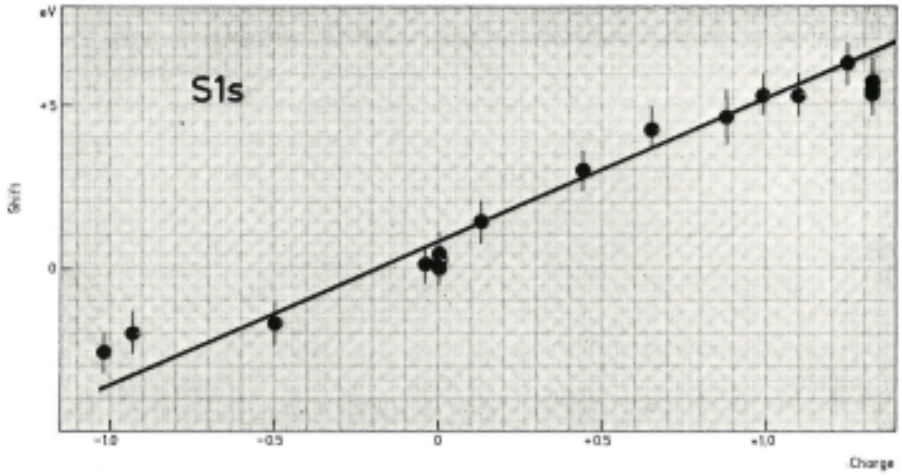

Figure 10: The experimental shift of the sulfur compounds versus the 'Pauling charge', explained in the text (from the first ESCA book [10, p.106]).

Fig:ShiftS3

locations, as illustrated in Fig.7. It was then realized that the shift was correlated to the chemical environment.

After the discovery of the double sulfur peak in thiosulfate, it was rapidly realized that the electron-spectroscopy method, developed by the Uppsala group, could be used for chemical analysis. ***The ESCA method – Electron Spectroscopy for Chemical Analysis – was born***.

In Fig.8 the experimental shifts for various sulfur compounds are displayed *versus* the traditional chemical valence or oxidation number. The results are somewhat scattered, and in particular there is a significant difference between organic and inorganic compounds. In this very simple model it is assumed that the electrons are completely transferred from the element with lower to that with higher electro-negativity. This is an oversimplification, since when the difference in electro-negativity is small, the bond has an appreciable covalent character. A simple refinement of the model is to assume that the bond is entirely ionic if the difference in electro-negativity is larger than 0.5 and entirely covalent if the

difference is smaller than 0.5 (in which case only one half of the charge in the ionic model is transferred). This leads to what is referred to as the *modified oxidation number*. It is found that the experimental shift is much better correlated to this number, as illustrated in Fig.9. Fig:ShiftS2

Taking into account the degree of covalency of the molecular bond in a more detailed manner, leads to what is known as the *Pauling charge*. By plotting the experimental shift *versus* this quantity, the correlation is even more pronounced (Fig.10). Fig:ShiftS3

It is clear from these illustrations that quite detailed information about the chemical environment can be deduced from the chemical shift in the spectrum, and this constitutes the fundament of the ESCA method.

4 Calculation of chemical shifts

sec:Calc

The chemical shift in the ESCA spectrum – or equivalently in the X-ray spectra – is caused by changes in the electron binding energies. Therefore, we shall here consider different ways of calculating the electron binding energy of an atom or a molecule – methods that can also be used to evaluate chemical shifts.

4.1 Single-particle picture

ec:SingPart

More detailed calculations of electron binding energies could not be performed until the 1960's, when sufficiently powerful computers became available. Essentially two methods were then developed,

- the Koopmans-theorem method and
- the ΔSCF method.

In the Hartree-Fock model the binding or removal energy of an electron is according to Koopmans' theorem [14] Koop33 equal to the negative of the orbital energy eigenvalue

$$\mathrm{BE} = -\varepsilon_{\mathrm{HF}}.$$

This assumes that the remaining electrons are unaffected by the removal or in other words that the *electron relaxation* is neglected. If some other SCF scheme is used, such as the Slater exchange approximation [15, 16] S151,S172 or variants thereof, the Koopmans' theorem is not exactly valid, but the non-validity of this theorem is easily corrected for.

In the ΔSCF method, separate self-consistent-field (SCF) calculations are performed of the system before and after the removal of the electron. In this way the electron relaxation is taken into account to a considerable degree.

Atomic self-consistent-field calculations

sec:SCF

In the early 1960's we performed in Uppsala extensive SCF calculation of atomic systems, using a modification of the Slater exchange approximation, as described in the first ESCA book [10, p.63, App.2] ESCA67. In those days full Hartree-Fock (HF) calculations with non-local

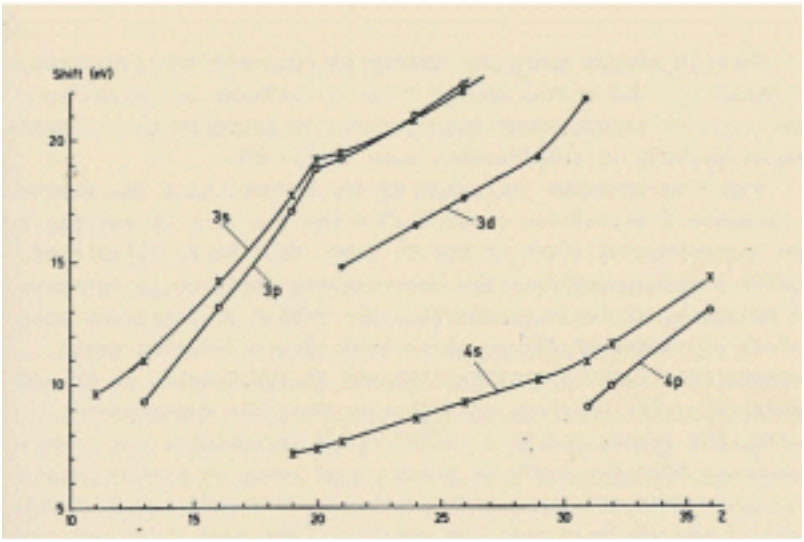

Figure 11: The shift of the 1s electron binding energy when an electron of an outer shell is removed to infinity (From Lindgren 1966 [17]).

Fig:SCFHole

exchange potential were rather expensive. In the Slater exchange approximation, the HF exchange is replaced by a *local* potential [15, 16]

$$V_{\rm Slex}(\boldsymbol{r}) = -\frac{3}{2}\Big(\frac{3}{\pi}\Big)\rho(\boldsymbol{r})^{1/3},$$

where $\rho(\boldsymbol{r})$ is the electron density. This represents the introduction of a *local-density approximation* (LDA), which is an important ingredient of the *density-functional theory* (DFT), which nowadays has been extremely popular in quantum chemistry.

Table 3: Electron binding energies of the argon atom (in eV)
(From the first ESCA book [10, App.2])

Shell	Koopmans	ΔSCF	Expt'l
1s	3240	3209	3203
2s	336	327	(320)
$2p_{1/2}$	261	250	247
$2p_{3/2}$	259	248	245

Tab:Argon

In the mid 1960's we introduced a modification of the Slater potential, referred to as the *optimized exchange potential* [18, 19],

$$V_{\rm Optex}(\boldsymbol{r}) = C\, r^{n/3}\, V_{\rm Slex}(\boldsymbol{r}),$$

where C and n are adjustable parameters, determined by minimizing the total energy of the atom. It was then found that the same parameter set, C=0.85 and n=1.15, could be used over essentially the entire periodic table (see the first ESCA book [10, p.66]). This potential is as easy to use as the original Slater approximation, but yields considerably better results. It is interesting to note that Slater five years later introduced the widely used *X-α approximation* [20, 16]

$$V_{\rm X\alpha}(\boldsymbol{r}) = \alpha\, V_{\rm Slex}(\boldsymbol{r}),$$

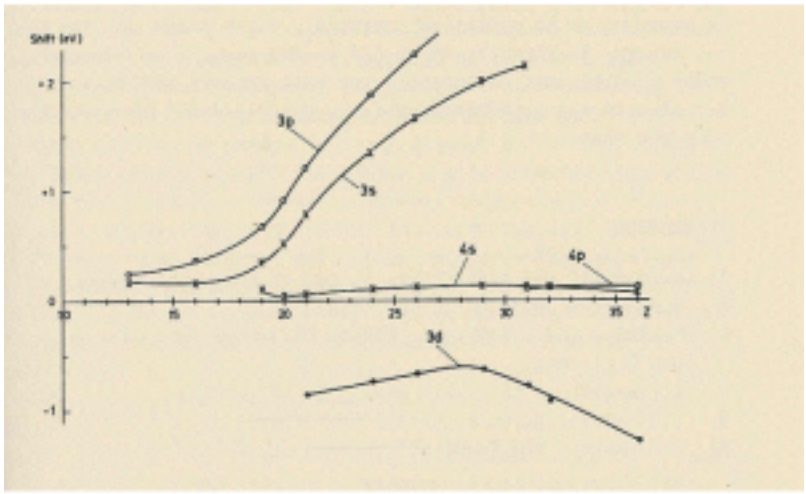

Figure 12: The shift of the Kα X-ray energy when an electron of an outer shell is removed to infinity (From Lindgren 1966 [17]). LiLeip65

Fig:SCFHole2

where the parameter α is determined from energy minimization. This is identical to our optimized potential with one of the parameters removed. In contrast to the optimized potential, the optimization in the X-α method has to be performed for each element separately.

As an example of the Koopmans and ΔSCF methods we consider the results of some of our early relativistic SCF calculation, displayed in Table 3. The difference between the Koopmans and the ΔSCF results represents the effect of the relaxation, which is seen to be quite appreciable. The remaining discrepancy between the ΔSCF and the experimental results, which is considerably smaller, represents higher-order many-body or electron-correlational effects. Tab:Argon

In Fig. 11 we display the result of our SCF calculations of the effect on the inner-shell binding energies due to the removal of one outer electron. The corresponding shifts in the Kα X-ray energy are displayed in Fig. 12. There we can see that the shift due to single ionization on the binding energy is of the order of 10-20 eV, while the corresponding shift of the X-ray energies is one order of magnitude smaller. This is in qualitative agreement with the early experimental results, illustrated in Tables 1 and 2 above. Fig:SCFHole Fig:SCFHole2 Tab:Linde Tab:Back

Atomic calculations of the kind discussed here can only give a qualitative picture of the process of chemical shifts in X-ray and photoelectron spectra. These calculations are based upon the extreme ionic model, where the electrons are removed to infinity. In reality we have to take into account the fact that the charge is mainly transferred to neighboring ions and that the chemical bonds are normally at least partly covalent, as discussed in section 2.2. sec:Interpret

For solids the effect of the crystal field can be taken into account by performing the summation over the ions of the crystal. The result of such a calculation is exhibited in Fig. 13 for the crystal of sodium thiosulfate, where the difference in binding energy of the inner core levels between the two sulfur ions is shown. It is found, as expected, that the crystal field largely cancels the effect of the pure ionic model, and reduces the total shift an order of magnitude. When compared with the experimental shift in this case, it is found that the 'effective charge' transferred from the central sulfur ion to its neighbors is of the order of 1.5 charge units, which is reasonable considering the covalency of the bond. Fig:Crystal

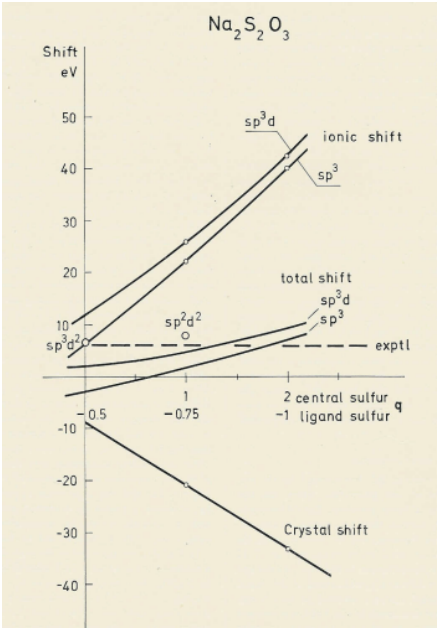

Figure 13: Ionic and crystal-field shift of the inner core levels between the two sulfur ions in sodium thiosulfate (from the first ESCA book [10, p.94]). ESCA67 Fig:Crystal

sec:MolCalc

Molecular calculations

Molecular calculations are considerably more complicated to perform than the corresponding atomic ones, and for that reason various semi-empirical methods for molecular calculations have been developed over the time. One of the most popular methods of this kind is CNDO (Complete Neglect of Differential Overlap), developed by Pople and coworkers in the 1960's [22, 23]. In Fig.14 the chemical shift evaluated by this method is compared with the observed one for a number of sulfur compounds. With a few exceptions, the agreement is found to be quite good. PopSeg65,Pople66 Fig:CNDO

Table 4: LCAO-SCF calculations of chemical shifts (eV)
(From Basch and Snyder 1969 [24]) BS69

Molecule	Calculated	Expt'l
CH_4	-8.3	-6.8
CH_3OH	-6.3	-4.7
CO	-2.8	-1.6
CO_2	0	0

Tab:MolSCF

More extensive *ab-initio* molecular calculations, using methods like SCF-LCAO (Linear Combination of Atomic Orbitals), became feasible in the late 1960's and early 1970's. One of the first chemical-shift calculation of this kind is that of Basch and Snyder in 1969 [24], using the Koopmans' theorem, and some of their results are shown in Table 4. BS69 Tab:MolSCF The agreement with experimental results is of the order of 20-30 %, which is reasonable, regarding the fact that relaxation and correlation effects are unaccounted for.

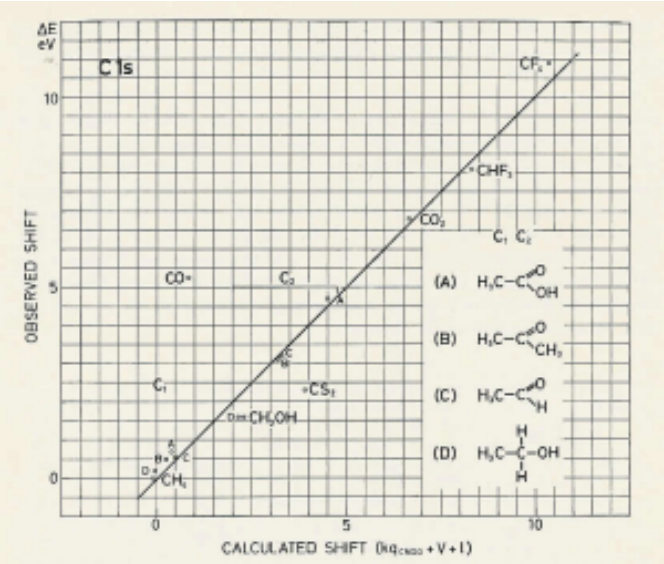

Figure 14: The chemical shift of some sulfur compounds evaluated by the CNDO method and compared with the experimental value (from the second ESCA book [21, p.118]). ESCA69 Fig:CNDO

4.2 Calculations beyond the single-particle picture

sec:MB

For more accurate calculations of electron binding energies and chemical shift is necessary to go beyond the single-particle picture and consider the full many-body problem in one way or the other. A large variety of methods have been developed over the time for this purpose, and it far beyond the scope of the present review to cover this field in any comprehensive way – only a few illustrations will be given. For further information the reader is referred to excellent reviews that are available in the literature [25, 26, 27, 28]. Nordfors91,Agren95,Agren91,AgrenCarr9

The molecular many-body schemes can be categorized as follows:

- Variational techniques, such as configuration interaction (CI) or multi-configuration self-consistent fields (MCSCF);
- Perturbative and iterative techniques, such as many-body perturbation theory (MBPT), Coupled-Cluster Approach (CCA) or Green's-function (GF) technique;
- Density-functional theory (DFT).

Variational techniques

In the variational methods, the wavefunction is constructed with a number of free parameters, which are determined by minimizing the total energy of the system. In the CI technique the wavefunction is expanded in configurations with fixed orbitals. This many-body technique has been frequently used since the 1960's. Nowadays millions of configurations can be handled, yielding quite good accuracy [29]. Agren83

In the MCSCF method also the orbitals are varied as in standard SCF, and normally only a limited number of configurations is used. In the CAS-MCSCF (Complete Active Space MCSCF) method, developed and extensively used by Per Siegbahn, Björn Roos and coworkers, tens of thousands of configurations can be handled [30, 31]. Sieg81,Roos80

Table 5: 1s binding energies for methane (eV)

Method	Bind.en	Ref.
CEPA	290.677	Meyer [35]
CPNO	290.701	Meyer [35]
CAS-MCSCF	290.689	P. Siegbahn [37]
Expt'l	290.707(3)	Gelius et al. [37]

Tab:Methane

In using variational techniques for determining electron binding energies, separate calculations have to be performed for the system before and after the removal of the electron in order to take the relaxation into account. Furthermore, methods of this type are not *size extensive* [32, 33], which implies that the energy does not scale properly with the size of the system. This can be compensated for in an approximate way, though, by means of the so-called Davidson correction [34].

As a first illustration to molecular many-body calculations we consider the $1s$ binding energy of methane, and some results are given in Table 5. The early calculations of Meyer [35] are impressive. They are made by (i) the so-called CEPA method (Coupled-Electron-Pair-Approximation) (see, for instance, [36, Ch.15]), which takes the electron pair correlation approximately into account, and (ii) what is referred to a 'pseudo natural orbitals' (PNO). In addition, a result obtained with the above-mentioned CAS-MCSCF method is included. The experimental result is obtained by Gelius et al. [37].

Perturbative and iterative methods

Perturbative schemes, such as the Rayleigh-Schrödinger, the Møller-Plesset (MP) or the linked-diagram expansion – the latter often referred to as the *Many-body Perturbation Theory* (MBPT) – are normally performed *order by order*. For real atoms or molecules such expansions usually converge quite slowly, and at the same time the number of terms (diagrams) needed to go beyond fourth order, say, is prohibitedly large (see, for instance the book by Lindgren and Morrison [36]). Therefore, it is very hard to perform accurate calculations in this way.

Instead of expanding the perturbation order by order, it is possible to separate the perturbations (using second quantization) into one-, two-, ... body parts, essentially corresponding to single, double, ... excitations in the wavefunction. These parts can be treated to arbitrary order by solving a set of coupled single-particle, two-particle, ... equations iteratively – which combined with the exponential Ansatz leads to the Coupled-Cluster Approach (CCA) [36, Ch.14]. The CCA is now a standard tool in molecular calculations, and 'cluster terms' up to quadruples (SDTQ) can routinely be handled (at least for limited basis sets) [33].

The single-particle contributions to the wavefunction can be used to modify the orbitals of the single determinant. Considering a closed-shell system for simplicity, this is indicated schematically in the upper part of Fig.15. Here, the thin lines represent the original (HF) and the thick lines the modified orbital. The large box (Σ) represents the single-particle contribution, which is of *self-energy* type with a single electron in the initial and final states. This self energy can be separated into *proper self energy* parts (Σ^*, represented by the small box) that cannot be separated further by cutting a single line [38]. This expansion generates orbitals that contain all single excitations of the wavefunction, which implies that they are *Brueckner or maximum-overlap orbitals* (BO) [39, 40, 41]. The energy eigenvalue

Table 6: Electron binding energies for lithium atom (atomic units)
(From Lindgren 1985 [Li85])

Level	HF	BO	Expt'l
2s	0.196 304	0.198 154	0.198 158
sp	0.128 637	0.130 221	0.130 246

Tab:Li

of the Brueckner orbital represents the corresponding removal energy [Li85,Ls02].

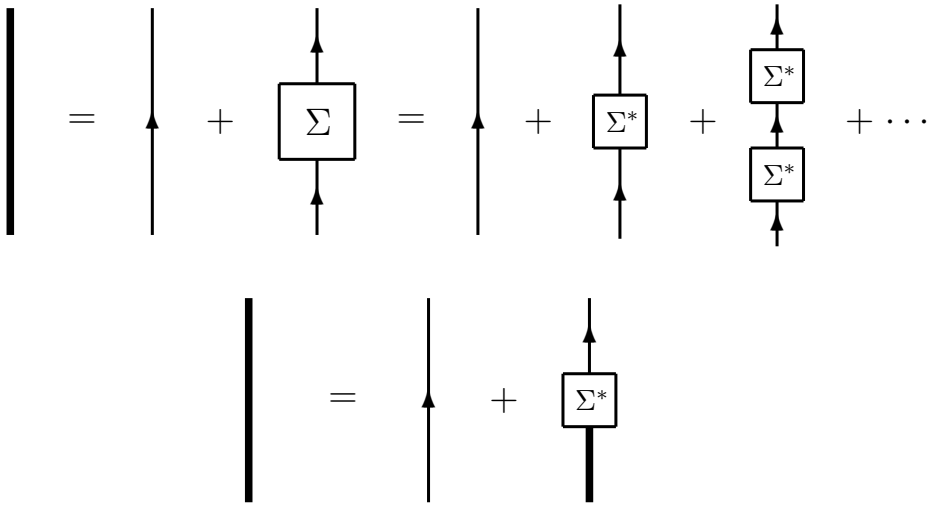

Figure 15: Graphical representation of the Dyson equation for the Brueckner or Dyson orbitals (thick lines). The thin lines represent unperturbed (HF) orbitals. The large box represents all single-particle effects of the wavefunction (complete self energy), and the small box represents the *proper* self-energy, defined in the text. This figure is also a representation of the Dyson equation for the single-particle Green's function (GF). The thin lines then represent the zeroth-order GF and the thick line the full GF.

Fig:Dyson

As an example of the process described, we consider the calculation on the lithium atom [Li85], and the result is shown in Table 6. The difference between the Hartree-Fock and Brueckner-orbital results represents the effect of relaxation and correlation. This is a coupled-cluster calculation with singles and doubles, and about 99% of the many-body effects (beyond Hartree-Fock) are accounted for. The residual effect is mainly due to the omitted three-body clusters.

Extensive relativistic many-body calculations of the inter-shell ionization energies and $K\alpha$ energies of atoms, including some QED effects, have recently been performed by Indelicato et al. [IBL98]. The impressingly good agreement between theory and experiment is illustrated for the $K\alpha_1$ energies in Fig. 16.

The perturbative expansion in Fig. 15 (upper part) can also be expressed as a *Dyson-type* equation, indicated in the bottom part of the figure, which is solved iteratively. It can be shown that this corresponds to the equation [wLS97,LiBr04]

$$h_0\,\phi(\boldsymbol{r}) + \int \mathrm{d}\boldsymbol{r}\,\Sigma^*(\boldsymbol{r},\boldsymbol{r}_1,\varepsilon)\,\phi(\boldsymbol{r}_1)\,\mathrm{d}^3\boldsymbol{r}_1 = \varepsilon\,\phi(\boldsymbol{r}),$$

which is also the equation for so-called *Dyson orbitals* [Mig67,Ortiz99]. Here, h_0 represents the hamiltonian for an electron moving in the nuclear field, and Σ^* is as before the proper self energy. This equation is equivalent to the corresponding equation for the *single-particle*

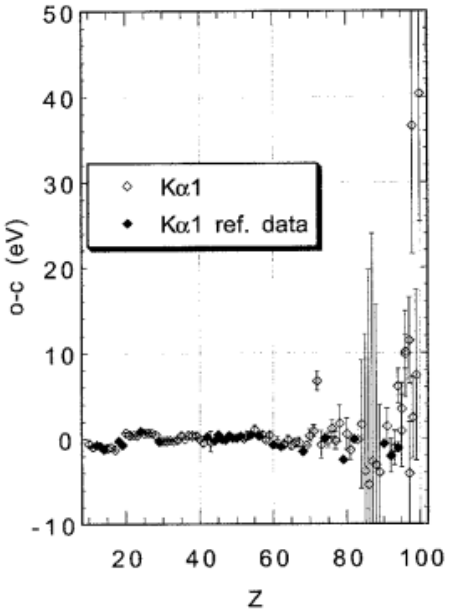

Figure 16: Difference between theory and experiment for the $K\alpha_1$ energies of various elements (from Indelicato, Buchard and Lindroth 1998 [44].

Fig:Lindroth

Table 7: 1s binding energies for N_2 (eV)

Method	Bind.en.	Ref.
CI	410.71	Ågren et al. [29]
GF	410.0	Shirmer et al. [49]
Expt'l	409.9	Gelius [50]

Tab:N2

Green's function (GF) [47, 38, 45],

$$G(\boldsymbol{r}', \boldsymbol{r}, \omega) = G_0(\boldsymbol{r}', \boldsymbol{r}, \omega) + \iint \mathrm{d}^3\boldsymbol{r}_1\, \mathrm{d}^3\boldsymbol{r}_2\, G_0(\boldsymbol{r}', \boldsymbol{r}_2, \omega)\, \Sigma^*(\boldsymbol{r}_2, \boldsymbol{r}_1, \omega)\, G(\boldsymbol{r}_1, \boldsymbol{r}, \omega),$$

where, G_0 represents the zeroth-order GF and G the full (perturbed) GF. The pole of the GF represents the electron binding energy, including correlation and relaxation. This equation can also be represented graphically as in the bottom line of Fig. 15. The relation between the perturbative and GF approaches is further discussed in ref. [46].

Inner-shell ionization spectra of some molecules have been studied using the fourth-order Green's-function technique by Schirmer et al. [49, 51], and the result for the 1s binding energy of N_2 is given in Table 7. There we have also included for comparison a CI calculation by Ågren et al. [29]. It has been argued that the Green's-function technique (as well as other iterative methods using the valence universality condition, mentioned above) would not be suitable for inner-shell ionization energies because of the strong relaxation [27]. The results of Shirmer at al. [49, 51] as well as those of Indelicato et al. [44] seem to demonstrate that this strong relaxation can nowadays be handled by such methods.

The process of inner-shell ionization is normally associated by a number of satellites in the spectrum, known as *shake-up lines*. Theoretically this is normally handled by means of the so-called *sudden approximation*, and extensive studies of this process have been performed (see, for instance, the review by Ågren and Carravetta [28]). The sudden approximation and its transition to the adiabatic process has also been studied particularly by Hedin et al. [52, 53].

Figure 17: Illustration of the Slater transition-state procedure, described in the text. Fig:TransState

Density-functional theory

In recent years remarkably accurate calculations have been performed of the electron binding energies of quite complicated molecules, using the density-functional theory (DFT). Essentially two schemes have here been developed:

- A generalization of the standard Kohn-Sham method, known as the Δ*Kohn-Sham method*, where separate DFT calculations are performed for the initial and final states, as in the ΔSCF method, mentioned above;
- A DFT calculation in combination with a generalization of the Slater transition state, which takes the relaxation into account to a high degree of accuracy.

Both these methods have been demonstrated to yield remarkable accuracy for the binding energies, including vibrational excitations – of the order of a few tenths of an eV. The first method was introduced by Triguero et al. [54] and is discussed also in a paper by Carniato and Millié [55], where several different methods for calculating core-electron binding energies are compared. In a paper by Birgersson et al. [56] the method is successfully applied also to some solids.

The second method can be illustrated by means of the original Slater transition state [16] (see Fig.17). If we know the total energy, $E(n)$, of a system as a function of the occupation number (n), treated as a continuous variable, we can estimate the binding energy of the least bound electron of a system with n_0 electrons by taking the derivative of the energy with respect to the occupation number at a point $n = n_0 - 1/2$, known as the *transition state*,

$$\mathrm{BE} = \mathrm{E(n_0)} - \mathrm{E(n_0 - 1)} \approx \Big(\frac{\partial \mathrm{E}}{\partial \mathrm{n}}\Big)_{\mathrm{n=n_0-1/2}}.$$

This approximation has been frequently applied in connection with the local exchange approximation of the Slater type.

The transition-state technique is also used with the more accurate exchange approximations, recently developed in the scope of density-functional theory (DFT). According to this theory, the ground-state energy of any electronic system is a unique functional of the electron density. This functional is not known, but better and better approximations are now being developed, based upon the local-density approximation (LDA) and various gradient approximations (GA).

Table 8: $1s$ binding energies for $C^2H_3 - C^1N$ Acetonitrile
(From Chong et al. 1997 [60])

	ΔSCF	MP2	Chong	Expt'l
C^1	293.24	292.07	292.78	292.60
C^2	293.46	292.36	292.85	292.88
N	405.23	404.71	405.49	405.58

Tab:DFT

Chong et al. [57, 58, 59, 60, 61, 62] have in recent years calculated extremely accurate electron binding energies using the Becke-Perdew density-functional approximation [63, 64] and a generalization of the Slater transition-state formula formula [65]

$$\mathrm{BE} \approx \frac{1}{4}\Big(\frac{\partial \mathrm{E}}{\partial \mathrm{n}}\Big)_{\mathrm{n}=\mathrm{n}_0} + \frac{3}{4}\Big(\frac{\partial \mathrm{E}}{\partial \mathrm{n}}\Big)_{\mathrm{n}=\mathrm{n}_0-2/3}.$$

As an illustration we consider the calculation on the molecule acetonitrile, $C^2H_3{-}C^1N$ (see Table 8). The second column shows the result of a ΔSCF calculation, the third column the result of second-order perturbation theory (MP2) and the fourth the DFT result of Chong et al. Similar results have been obtained by the same authors for a large number of other molecules. The results are quite remarkable and show that accurate DFT calculations yield considerable more accurate results than ΔSCF and (low-order) perturbation theory. The DFT calculations are performed in a self-consistent way but are claimed to be only moderately more time consuming than standard Hartree-Fock calculations.

5 Summary and Conclusions

The chemical shifts in X-ray spectroscopy were detected and qualitatively interpreted some 80 years ago. The corresponding shifts in core-electron spectroscopy were detected and interpreted 40 years later. Quantitative evaluation of the core-electron binding energies and shifts became possible when sufficiently powerful computers were available in the 1960's. During the past four decades a large number of more or less sophisticated computational methods have been developed, and it is now possible to evaluate the binding energies – including vibrational levels and the satellite structure – and chemical shifts with an accuracy of the order of 0.1 eV, also for relatively complex molecules. Therefore, the combination of accurate experimental and theoretical investigations can now yield valuable information about molecular structure and dynamics.

References

Sieg31 [1] M. Siegbahn, *Spektroskopie der Röntgenstrahlen* (Springer, Berlin, 1931).

Lindh21 [2] A. Lindh, Z. Phys. **6**, 303 (1921).

Berg20 [3] J. Bergengren, Z. Phys. **3**, 247 (1920).

Back25 [4] E. Bäcklin, Z. Phys. **3**3, 547 (1925).

LL24 [5] A. Lindh and O. Lundquist, Ark. Mat. Astr. o. Fys. **1**8, 34 (1924).

LL24a [6] A. Lindh and O. Lundquist, Ark. Mat. Astr. o. Fys. **1**8, 35 (1924).

Ray25 [7] B. B. Ray, Phil. Mag. **4**9, 168 (1925).

Wenz22 [8] G. Wenzel, Naturwiss **1**0, 464 (1922).

Cost24 [9] D. Coster, Z. Phys. **2**5, 83 (1924).

ESCA67 [10] K. Siegbahn, C. Nordling, A. Fahlman, R. Nordberg, K. Hamrin, J. Hedman, G. Johansson, T. Bergmark, S.-E. Karlsson, I. Lindgren, and B. Lindberg, *ESCA. Atomic, molecular and solid state structure studied by means of electron spectroscopy* (Almqvist-Wiksells, Uppsala, 1967).

SNS58 [11] E. Sokolowski, C. Nordling, and K. Siegbahn, Phys. Rev. **1**10, 776 (1958).

HNS64 [12] S. Hagström, C. Nordling, and K. Siegbahn, Z. Phys. **1**78, 439 (1964).

NSS57 [13] C. Nordling, E. Sokolowski, and K. Siegbahn, Phys. Rev. **1**05, 1676 (1957).

Koop33 [14] T. Koopmans, Physica **1**, 104 (1933).

Sl51 [15] J. C. Slater, Phys. Rev. **8**1, 385 (1951).

Sl72 [16] J. Slater, Adv. Quantum Chem. **6**, 1 (1972).

LiLeip65 [17] I. Lindgren, in *Röntgenspektren in chemische Bindung*, edited by A. Meisel (Physikalisch-Chemisches Institut der Karl-Marx-Universität, Lepzig, 1966).

Li65 [18] I. Lindgren, Phys. Lett. **1**9, 382 (1965).

RosL68 [19] A. Rosén and I. Lindgren, Phys. Rev. **1**76, 114 (1968).

SWW69 [20] J. C. Slater, T. M. Wilson, and J. H. Wood, Phys. Rev. **1**79, 28 (1969).

ESCA69 [21] K. Siegbahn, C. Nordling, G. Johansson, J. Hedman, P. F. Hedén, K. Hamrin, U. Gelius, T. Bergmark, L. O. Werme, R. Manne, and Y. Baer, *ESCA applied to free molecules* (North-Holland, Amsterdam-London, 1969).

PopSeg65 [22] J. A. Pople and G. A. Segal, J. Chem. Phys. **4**3, S136 (1965).

Pople66 [23] J. A. Pople and G. A. Segal, J. Chem. Phys. **4**4, 3289 (1966).

BS69 [24] H. Basch and L. C. Snyder, Chem. Phys. Lett. **3**, 333 (1969).

Nordfors91 [25] D. Nordfors, A. Nilsson, N. Mårtensson, S. Svensson, U. Gelius, and H. Ågren, J. Electr. Spect. Rel. Phen. **5**6, 117 (1991).

Agren95 [26] F. Gel'mukhanov and H. Ågren, J. Chem. Phys. **1**03, 5848 (1995).

Agren91 [27] H. Ågren, Int. J. Quantum Chem. **3**9, 455 (1991).

AgrenCarr92 [28] H. Ågren and V. Carravetta, Int. J. Quantum Chem. **4**2, 685 (1992).

Agren83 [29] H. Ågren, R. Arneberg, J. Müller, and R. Manne, Chem. Phys. **8**3, 53 (1983).

Sieg81 [30] P. E. M. Siegbahn, J. Almlöf, A. Hedberg, and B. O. Roos, J. Chem. Phys. **7**4, 2384 (1981).

Roos80 [31] B. O. Roos, P. R. Taylor, and P. E. M. Siegbahn, Chem. Phys. **4**8, 157 (1980).

PBS76 [32] J. A. Pople, J. S. Binkley, and R. Seeger, Int. J. Quantum Chem. **S**10, 1 (1976).

BP78 [33] R. J. Bartlett and G. D. Purvis, Int. J. Quantum Chem. **1**4, 561 (1978).

David74 [34] E. R. Davidson, in *The World of Quantum Chemistry*, edited by R. Daudel and B. Pullman (Reidel, Dordrecht, 1974).

Meyer73 [35] W. Meyer, J. Chem. Phys. **5**8, 1017 (1973).

LM86 [36] I. Lindgren and J. Morrison, *Atomic Many-Body Theory* (Second edition, Springer-Verlag, Berlin, 1986).

Gelius85 [37] L. Asplund, U. Gelius, S. Hedman, K. Helenelund, K. Siegbahn, and P. E. M. Siegbahn, J. Phys. B **1**8, 1569 (1985).

FW71 [38] A. L. Fetter and J. D. Walecka, *The Quantum Mechanics of Many-Body Systems* (McGraw-Hill, N.Y., 1971).

Br57 [39] W. Brenig, Nucl. Phys. **4**, 363 (1957).

Lo62 [40] P.-O. Löwdin, J. Math. Phys. **3**, 1171 (1962).

LLM76 [41] I. Lindgren, J. Lindgren, and A.-M. Mårtensson, Z. Phys. A **2**79, 113 (1976).

Li85 [42] I. Lindgren, Phys. Rev. A **3**1, 1273 (1985).

Ls02 [43] I. Lindgren and S. Salomonson, Int. J. Quantum Chem. **9**0, 294 (2002).

IBL98 [44] P. Indelicato, S. Bouchard, and E. Lindroth, Eur. Phys. J. D **3**, 29 (1998).

WLS97 [45] H. Warston, I. Lindgren, and S. Salomonson, Phys. Rev. A **5**5, 2757 (1997).

LiBr04 [46] I. Lindgren, *Löwdin Memorial III* (Elsivier, ADDRESS, 2004).

Mig67 [47] A. B. Migdal, *Theory of Finite Fermi Systems and Applications to Atomic Nuclei* (Interscience, Wiley, N.Y., London, Sidney, 1967).

Ortiz99 [48] J. V. Ortiz, Adv. Quantum Chem. **3**5, 33 (1999).

Schirmer87 [49] G. Angonoa, O. Walter, and J. Schirmer, J. Chem. Phys. **8**7, 6789 (1987).

Gelius74 [50] U. Gelius, J. Electr. Spect. Rel. Phen. **5**, 985 (1974).

Schirmer87a [51] J. Schirmer, G. Angonoa, S. Svensson, D. Nordfors, and U. Gelius, J. Phys. B **2**0, 6031 (1987).

Hedin02 [52] L. Hedin and J. D. Lee, J. Electr. Spect. Rel. Phen. **1**24, 289 (2002).

Hedin99 [53] J. D. Lee, O. Gunnarsson, and L. Hedin, Phys. Rev. B **6**0, 8034 (1999).

Triguero99 [54] L. Triguero, O. Plashkevych, L. G. M. Pettersson, and H. Ågren, J. El. Spect. Rel. Phen. **1**84, 195 (1999).

CarnMill02 [55] S. Carniato and P. Millié, J. Chem. Phys. **1**16, 3521 (2002).

BABA03 [56] M. Birgersson, C.-O. Almbladh, M. Borg, and J. N. Andersson, Phys. Rev. B **6**7, 045402 (2003).

Chong95 [57] D. P. Chong, Chem. Phys. Letters **2**32, 486 (1995).

Chong95a [58] D. P. Chong, J. Chem. Phys. **1**03, 1842 (1995).

Chong96 [59] D. P. Chong, C.-H. Hu, and P-Duffy, Chem. Phys. Letters **2**49, 491 (1996).

Chong97 [60] C. Bureau, D. P. Chong, G. Lécayon, and J. Delhalle, J. El. Spect. Rel. Phen. **8**3, 227 (1997).

Chong98 [61] D. P. Chong and C.-H. Hu, J. Chem. Phys. **1**08, 8950 (1998).

Chong02 [62] D. P. Chong, P. Aplincourt, and C. Bureau, J. Phys. Chem. A **1**06, 356 (2002).

Be88 [63] A. D. Becke, Phys. Rev. A **3**8, 3098 (1988).

Perd86 [64] J. P. Perdew, Phys. Rev. B **3**3, 8822 (1986).

WGS75 [65] A. R. Williams, R. A. deGroot, and C. B. Sommers, J. Chem. Phys. **6**3, 628 (1975).